ACS central science

Open Access

http://pubs.acs.org/journal/acscii

Article

Pinpointing the Onset of Water Harvesting in Reticular Frameworks from Structure

Ha L. Nguyen, Andrea Darù, Saumil Chheda, Ali H. Alawadhi, S. Ephraim Neumann, Lifen Wang, Xuedong Bai, Majed O. Alawad, Christian Borgs, Jennifer T. Chayes, Joachim Sauer,* Laura Gagliardi,* and Omar M. Yaghi*

Cite This: https://doi.org/10.1021/acscentsci.4c01878

Read Online

ACCESS | Metrics & More | Article Recommendations | Supporting Information

ABSTRACT: Covalent organic frameworks (COFs) have emerged as promising atmospheric water harvesters, offering a potential solution to the pressing global issue of water scarcity, which threatens millions of lives worldwide. This study presents a series of 2D COFs, including HCOF-3, HCOF-2, and a newly developed structure named COF-309, designed for optimized water harvesting performance with a high working capacity at low relative humidity. To elucidate their water sorption behavior, we introduce a hydrophilicity index directly linked to intrinsic properties, such as the strength and spatial density of adsorptive sites. This index is mathematically correlated to the step of water adsorption isotherms. Our correlation provides a predictive tool that extends to other microporous COFs and metal−organic frameworks, significantly enhancing the ability to predict their onset positions of water adsorption isotherms based on structural characteristics. This advancement holds the potential to guide the development of more efficient materials for atmospheric water harvesting.

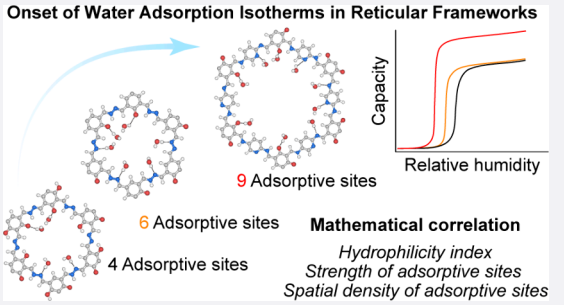

INTRODUCTION

Metal−organic frameworks (MOFs) and covalent organic frameworks (COFs) have emerged as promising materials for water harvesting from air, providing the potential to alleviate the global water crisis.[1−13] A practical water harvesting material must exhibit at least two important water uptake properties. First, a steep water uptake behavior so that minimal variation in pressure or temperature would be required to collect the harvested water.[7,14] Second, an onset of water uptake—a position corresponding to approximately 50% of water sorption capacity—at a relative humidity (RH) matching the prevailing humidity level in the region of interest.[15] While high crystallinity directly governs the steepness of water uptake, predicting the relative humidity at which the onset occurs is heretofore underdeveloped. Herein, we use COFs, which exhibit a highly tunable structure, high crystallinity, chemical stability, and versatile functionalization, as exemplars for how to determine *a priori* the onset of water harvesting from a given porous framework structure. Specifically, we find, contrary to the prevailing understanding, that the density of adsorptive sites (the number of adsorptive sites per unit area or volume) is a vital component in determining the onset position. We derive a mathematical relationship between the onset and the density of adsorptive sites as well as their strength, serving as a predictive descriptor of the water onset position in new microporous COFs and MOFs. Consistent with our newly developed equation, we report a novel water-harvesting COF that demonstrates an exceptional water uptake capacity and a low onset position.

RESULTS AND DISCUSSION

COF Synthesis, Characterization, and Their Water Sorption. Among the COFs investigated for water harvesting, 2D honeycomb (**hcb**) COFs with hydrazine linkages, such as AB-COF and COF-480-hydrazide,[6,7] exhibit promising water sorption behavior. However, their imine-bonded structures are prone to hydrolysis. In our efforts to make COFs that take up water at low relative humidity, combined with good water sorption stability upon cycling, we investigated three isoreticular **hcb** frameworks: the previously reported HCOF-3,[16] HCOF-2,[16] and a new COF which we named COF-309 (Figure 1).

HCOF-3 and HCOF-2 were synthesized using modified literature procedures.[16] COF-309 was prepared by mixing solids of 2,4-dihydroxy-1,3,5-triformylbenzene (TFB-2OH) and 2,5-diaminopyridine (DAPy) in a solution of dioxane, 1,2,4-trichlorobenzene, and aqueous 6 M acetic acid. While

Received: November 3, 2024
Revised: February 4, 2025
Accepted: February 5, 2025

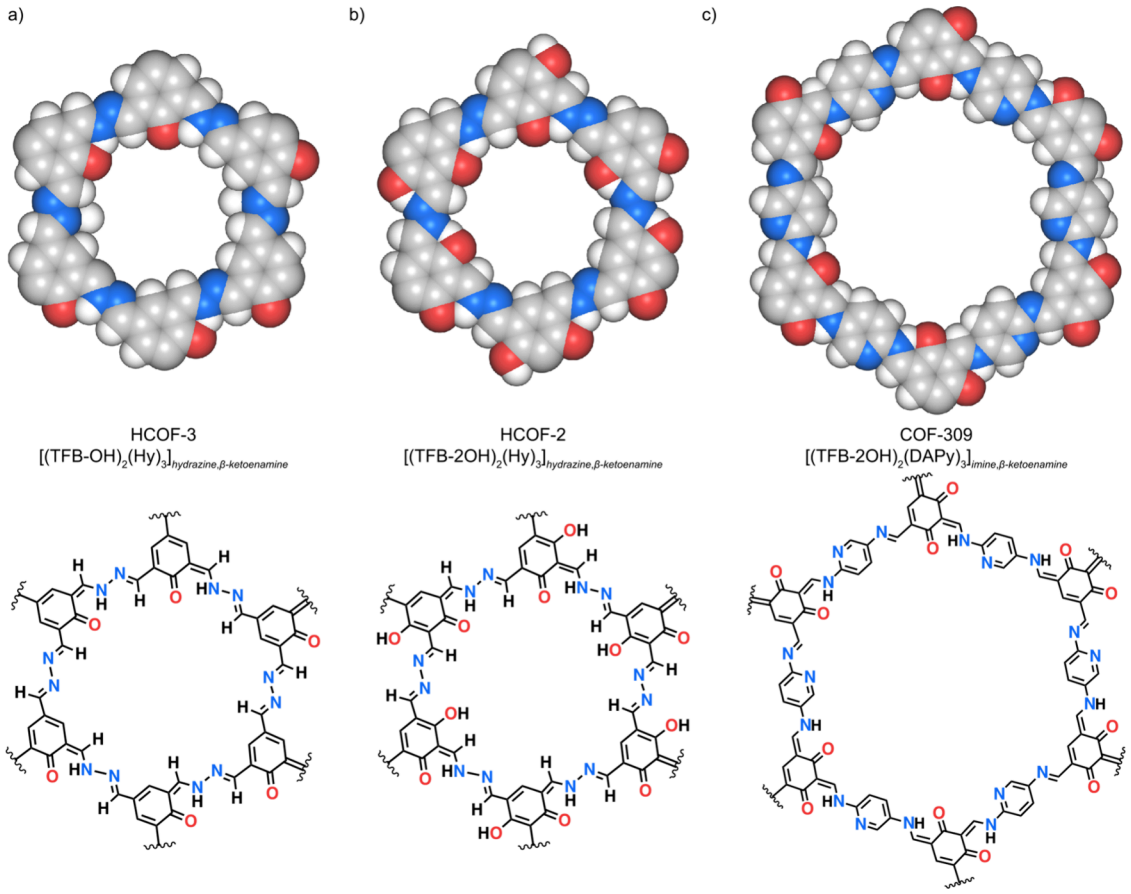

Figure 1. Space filling models and chemical structures corresponding to the single pore fragments of the isoreticular COFs in this study. (a, b) HCOF-3 $\{[(\text{TFB-OH})_2(\text{Hy})_3]_{hydrazine,\beta\text{-ketoenamine}}$; TFB-OH = 2-hydroxy-1,3,5-triformylbenzene, Hy = hydrazine$\}$ and HCOF-2 $\{[(\text{TFB-2OH})_2(\text{Hy})_3]_{hydrazine,\beta\text{-ketoenamine}}$; TFB-2OH = 2,4-dihydroxy-1,3,5-triformylbenzene$\}$ each comprised of hydrazine and β-ketoenamine linkages. (c) COF-309 $\{[(\text{TFB-2OH})_2(\text{DAPy})_3]_{imine,\beta\text{-ketoenamine}}$; DAPy = 2,5-diaminopyridine$\}$ composed of imine and β-ketoenamine linkages. Space filling model color code: C, gray; O, red; N, blue; H, light gray.

these solvents were chosen to ensure optimal solubility and reaction conditions in our proof-of-concept study, we think that exploring greener alternatives (ethanol, water, or other environmentally benign media) is crucial for scaling up. We obtained COF-309 in 96% yield within 3 h by using a microwave-assisted synthesis at 140 °C [Supporting Information (SI) Note 1]. This method indicates a potential for future scalability of COF-309 production.[17,18] The three COFs were characterized by Fourier-transform infrared spectroscopy (FT-IR), cross-polarization magic angle spinning ^{13}C nuclear magnetic resonance (^{13}C CP-MAS NMR), elemental analysis (EA), scanning electron microscopy (SEM), thermal gravimetric analysis (TGA), powder X-ray diffraction (PXRD), transmission electron microscopy (TEM), structural optimization using density functional theory (DFT), N_2 sorption, and H_2O sorption (SI Notes 1−3, Table S1, and Figures S1−S27).

In evaluating the water uptake behavior of these COFs, we made an unexpected observation. The ratios of hydrazine (which contains 2 adjacent imine functional groups) and β-ketoenamine moieties in HCOF-3 and HCOF-2 are 2:1 and 1:2, respectively. These ratios can only be verified using single-crystal X-ray analysis. Unfortunately, HCOF-2 and HCOF-3 did not crystallize as single crystals, so these ratios remain theoretical. Based on a higher number of more hydrophilic β-ketoenamines in HCOF-2, we anticipated its water onset position to shift to a lower relative humidity than that of HCOF-3. However, the water onset position in HCOF-2 was observed to shift to 32% RH from 23% RH in HCOF-3 (Figure 2).

To gain insight into the chemical reasons for this unexpected behavior, we performed DFT calculations with periodic boundary conditions on the COF unit cell (SI Note 3 and Note 4). We computed the strength of the binding of water to each functional group in the COFs and identified the number of potential adsorptive sites in each pore. The functional groups, ranked by their water binding strength (DFT calculations with the SCAN-D3BJ functional) from highest to lowest, are carbonyl ($\Delta E_{\text{Carbonyl-w}} = -16$ kcal mol^{-1}) greater than imine ($\Delta E_{\text{Imine-w}} = -10$ kcal mol^{-1}) greater than hydroxyl ($\Delta E_{\text{Hydroxyl-w}} = -6$ kcal mol^{-1}). To assess their nucleation ability, we compared these calculated water binding energies to those of two water molecules placed at the center of the COF pore, not interacting with the framework ($\Delta E_{\text{w-w}} = -9.4$ kcal mol^{-1}). We propose that functional groups should yield a water binding energy higher than $\Delta E_{\text{w-w}}$ to be considered as adsorptive sites. These calculations suggested HCOF-3 to have 6 adsorptive sites (2 carbonyl and 4 imine) but HCOF-2 to have only 4 adsorptive sites (2 carbonyl and 2 imine) in each pore fragment (Figure 3). The lower number of adsorptive sites found in HCOF-2 is due to the tautomerization of half of the β-ketoenamine functional groups, as computed using DFT (SI Note 3). The degrees of tautomerism in HCOF-3 and

https://doi.org/10.1021/acscentsci.4c01878
ACS Cent. Sci. XXXX, XXX, XXX−XXX

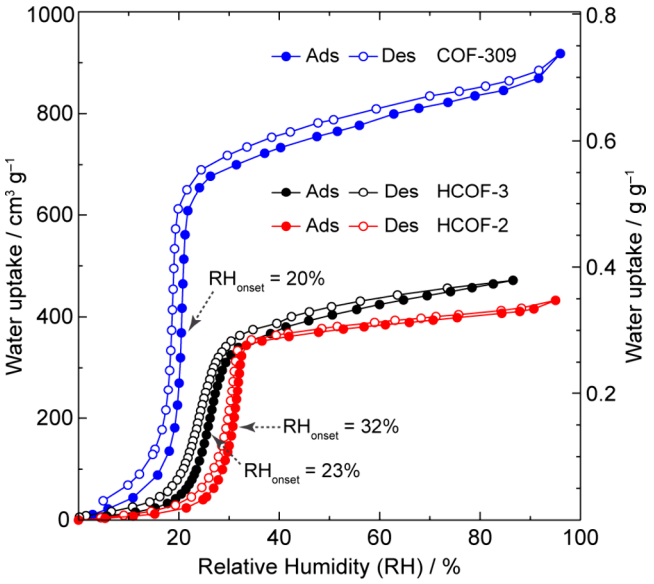

Figure 2. H_2O sorption measurements of HCOF-2, HCOF-3, and COF-309 at room temperature with onset positions at 32% RH, 23% RH, and 20% RH, respectively. COF-309 exhibits a total water uptake capacity of 0.74 g_{water} g_{COF}^{-1}.

HCOF-2 are 100% and 50%, respectively, based on DFT simulations. The hydroxyl groups were not found to be potential adsorptive sites because their water binding was weakened by hydrogen bond interactions with adjacent imine groups (SI Note 4 and Figures S28–S32). This results in the fact that the hydroxyl groups in HCOF-2 do not adsorb water molecules. The lower number of adsorptive sites in HCOF-2 thus leads to its shift to a higher water onset position.

Given these findings, we hypothesized that increasing the number of adsorptive sites with water binding energies larger than ΔE_{w-w} will shift the onset position of the water adsorption isotherm to a lower relative humidity. Therefore, we designed COF-309, which features 9 adsorptive sites in each pore fragment (4 carbonyl, 2 imine, and 3 pyridine; $\Delta E_{Pyridine-w} = -10$ kcal mol^{-1}; Figure 3).

COF-309 exhibited a Brunauer–Emmett–Teller surface area of 1698 m^2 g^{-1} with a pore size distribution at 15.3 Å (Figures S20 and S21) and exceptional water stability (Figures S21 and S22). Its water isotherm, measured at 25 °C, showed a steep step with the onset position at 20% RH and a total water uptake capacity of 0.74 g_{water} g_{COF}^{-1} (Figure 2). Additionally, water isotherms measured at 35 and 45 °C showed a negligible loss of the total water uptake capacity (Figure S23). The isosteric heat of adsorption ($\overline{\Delta H_{ads}}$) of COF-309 was calculated using the Clausius–Clapeyron equation which gave an average value of 48.1 kJ mol^{-1} (11.47 kcal mol^{-1}, Figure S24). Gibbs ensemble Monte Carlo simulations further corroborated the water sorption behavior observed in these COFs (SI Note 4 and Figures S26 and S27).

We performed cycling experiments to evaluate the long-term utilization of COF-309 under simulated application conditions. The water isobaric desorption of COF-309 was measured at a water vapor pressure of 1.70 kPa (corresponding to 40% RH at 30 °C) to probe the suitable regeneration temperature (Figure S33), allowing us to determine its desorption temperature of 60 °C. The adsorption–desorption experiments were then conducted under isobaric conditions with a temperature swing between 30 and 60 °C to trigger the release of 0.52 g_{water} g_{COF}^{-1} (Figure S34). This value is the highest water working capacity among reported water harvesting COFs. It also surpasses that of established water harvesting MOFs such as CAU-10,[19] MIL-160,[20] Al-fumarate,[21] MOF-303,[22] MOF-LA2-1(furan),[23] and MOF-LA2-2(furan)[23] and is comparable to MOF-LA2-1(pyrazole).[24] More importantly, the water working capacity of COF-309 remained almost unchanged after at least 170 water adsorption–desorption cycles (Figure S34). It should be noted that, while COF-309 and HCOF-2 are stable under water adsorption–desorption experiments, HCOF-3 is unstable under similar conditions (Figure S7).

Hydrophilicity Index. The water adsorption isotherms of the COFs studied in this work prompted a detailed examination of the framework properties governing the onset position in water harvesting COFs and MOFs. Particularly, a smaller shift in the onset position was observed between COF-309 (9 adsorptive sites, RH$_{onset}$ = 20%) and HCOF-3 (6 adsorptive sites, RH$_{onset}$ = 23%) in contrast to that between

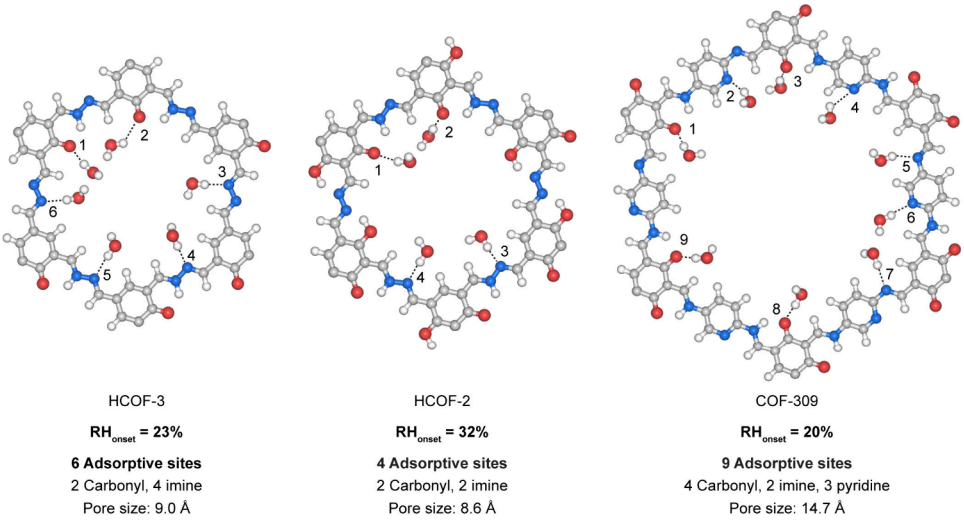

Figure 3. Computed water adsorptive sites in HCOF-3, HCOF-2, and COF-309 exhibiting 6, 4, and 9 water adsorptive sites in each pore fragment, respectively. Color code: C, gray; O, red; N, blue; H, light gray.

https://doi.org/10.1021/acscentsci.4c01878
ACS Cent. Sci. XXXX, XXX, XXX–XXX

HCOF-3 and HCOF-2 (4 adsorptive sites, RH_{onset} = 32%) despite a larger difference in the number of adsorptive sites between COF-309 and HCOF-3.

Generally, water adsorption in COFs and MOFs occurs in two stages: the first "seeding" stage, characterized by adsorption of primary water molecules onto the framework adsorptive sites, followed by the "pore-filling" stage where secondary water molecules form intermolecular hydrogen-bonded networks with the primary water molecules.[1,2,10,14,19] We hypothesized that a high density of adsorptive sites within sufficient proximity would favor hydrogen bonding of the secondary water molecules, facilitating the formation of continuous networks between isolated water clusters formed at the adsorptive sites.

We sought to establish a correlation between the onset position of the water adsorption isotherms of microporous COFs and MOFs and the strength and spatial density of their adsorptive sites. We defined the "hydrophilicity index" (i_H; a numerical value that represents a material's ability to interact with water, considering factors such as the number of adsorptive sites and the strength of their interactions with water) for each framework (eq 1)

$$i_H = \frac{N_{ads}}{S_A} \exp\left(-\frac{\overline{\Delta H_{ads}}}{RT}\right) \quad (1)$$

where N_{ads} is the number of adsorptive sites per one unit cell (details of N_{ads} calculations are provided in SI Note 5); $\overline{\Delta H_{ads}}$ is the average isosteric heat of water adsorption (kJ mol^{-1}), experimentally determined using the Clausius−Clapeyron relationship, which relates to the strength of the adsorptive sites; R is the ideal gas constant (J mol^{-1} K^{-1}); T is the temperature at which the isotherm is measured (K); S_A is the theoretical surface area per unit cell (m^2) calculated using N_2 probe radius (1.82 Å)—theoretical surface area is chosen to minimize deviations in calculations caused by low crystallinity (i.e., low experimental surface area). The hydrophilicity index can be standardized (i.e., made unitless) by multiplying by a factor of 1 × m^2.

For several microporous water harvesting COFs[4,6,7,10,25] and MOFs,[14,20,22−24,26,27] the i_H of the framework can be used to calculate its onset position of water adsorption (eq 2):

$$RH_{onset} = (i_H)^{-a} = \left(\frac{N_{ads}}{S_A} \exp\left(-\frac{\overline{\Delta H_{ads}}}{RT}\right)\right)^{-a} \quad (2)$$

RH_{onset}, defined as $\frac{p_{onset}}{p_{sat}}$ (where p_{onset} is the partial pressure of water vapor in kPa and p_{sat} is the saturated vapor pressure of water in kPa), represents the onset position of the water sorption isotherm (%). The onset positions of the water adsorption isotherms of MOFs and COFs were found to correlate with their hydrophilicity indices (Figure 4). Detailed methods for determining the hydrophilicity index and number of adsorptive sites are described in the SI (Note 5, Figures S35−S38, and Tables S2 and S3). As an example, we provided step-by-step calculation of the hydrophilicity index for MOF-801.[1] Additionally, we included an Excel file with calculations of the hydrophilicity indexes for various MOFs and COFs. Among water harvesting COFs, COF-309 stands out as a benchmark structure, exhibiting the lowest onset position at 20% RH. It is noted that we selected framework structures from the literature based on their high performance in atmospheric water harvesting, characterized by high water capacity and low onset of water sorption. Despite their structural diversity, their hydrophilicity indices correlate well with the onset of water harvesting. This demonstrates the broad applicability of our equation in predicting the onset of water harvesting for various framework structures.

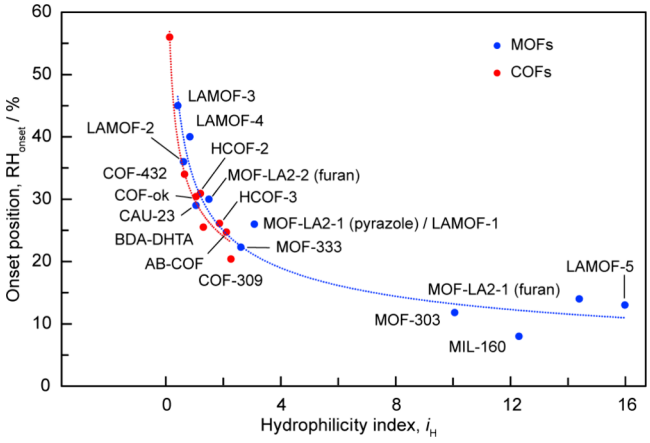

Figure 4. Correlation between the onset position of the water adsorption isotherms of microporous COFs and MOFs to their hydrophilicity index (i_H). As i_H increases, the onset position of the water adsorption isotherms of the COFs/MOFs reduces, shifting to a lower relative humidity.

Equation 2 can be rearranged to eq 3 to give insights into the thermodynamic origins of the proposed correlation. The nature and number of adsorptive sites effectively govern the free energy for water adsorption in the pores of the COF/MOF. The presence of strong adsorptive sites minimizes the enthalpy of water adsorption, while a higher density of these sites along the pore wall increases the configurational entropy of water molecules adsorbed within the framework. The constant parameter a (unitless) is characteristic of the class of microporous structure (COF or MOF) that may account for the long-range interactions of the adsorbed water molecules with the framework.

$$RT \ln(RH_{onset}) = RT \ln\left(\frac{p_{onset}}{p_{sat}}\right) = a(\overline{\Delta H_{ads}}) - aRT \ln\left(\frac{N_{ads}}{S_A}\right) \quad (3)$$

The calculation of i_H is not limited to the use of experimental $\overline{\Delta H_{ads}}$ but can also be approximated using estimated electronic energies of hydrogen bonds formed between water molecules and various functional groups (OLSA theory—Omar−Lac Ha−Saumil−Ali theory, SI Note 6 and Table S5). However, i_H can be more accurately calculated by determining the strength of individual adsorptive sites from more accurate calorimetric measurements or computational studies. It should be noted that we do not intend to use the i_H equation to describe the complexity of the water adsorption and desorption pathways within the pores of reticular structures. Readers are encouraged to refer to computational simulations reported in the literature.[28,29]

https://doi.org/10.1021/acscentsci.4c01878
ACS Cent. Sci. XXXX, XXX, XXX−XXX

CONCLUSION

We report the synthesis, characterization, and water sorption properties of a series of 2D COFs based on imine and β-ketoenamine linkages: HCOF-3, HCOF-2, and COF-309. HCOF-3 and HCOF-2, comprising 6 and 4 adsorptive sites, respectively, exhibit water onset positions at 23% and 32% RH, respectively. In contrast, our newly designed COF-309, having 9 adsorptive sites, displays a step-shaped water sorption isotherm with an onset position at 20% RH. Under isobaric conditions (p_{water} = 1.70 kPa) and a temperature swing between 30 and 60 °C, COF-309 exhibits a water working capacity of 0.52 g_{water} g_{COF}^{-1} and it is stable for at least 170 water adsorption−desorption cycles. The outstanding water sorption behavior of COF-309 can be attributed to the large pore volume, high spatial density, and strength of the adsorptive sites, which is supported by computational simulations. We derived a correlation between the strength and density of adsorptive sites for microporous reticular frameworks (COFs and MOFs) that successfully predicts the onset position of their respective water adsorption isotherms. Our proposed hydrophilicity index can be used to accelerate the design of new water harvesting frameworks by allowing a quick evaluation of their water onset positions. In conclusion, this work presents a novel, high-performing water harvesting framework (COF-309) with high water uptake capacity and an onset position at low relative humidity. Additionally, we introduce an effective descriptor (hydrophilicity index equation) for predicting the onset positions in water adsorption isotherms. Our equation can be applied to a wide range of microporous framework structures used in atmospheric water harvesting.

ASSOCIATED CONTENT

Supporting Information

The Supporting Information is available free of charge at https://pubs.acs.org/doi/10.1021/acscentsci.4c01878.

Synthesis and characterization of COFs including EA, FT-IR spectroscopy, NMR spectra, SEM, TGA, PXRD data, TEM, computational simulations, gas uptake measurements, and water isotherms (PDF)
Crystallographic information file for HCOF-2 (CIF)
Crystallographic information file for HCOF-3 (CIF)
Crystallographic information file for COF-309 (CIF)
Calculations of the hydrophilicity indexes for various MOFs and COFs (XLSX)

AUTHOR INFORMATION

Corresponding Authors

Joachim Sauer − *Institut für Chemie, Humboldt-Universität zu Berlin, Berlin 10099, Germany;* orcid.org/0000-0001-6798-6212; Email: js@chemie.hu-berlin.de

Laura Gagliardi − *Department of Chemistry, Pritzker School of Molecular Engineering, and Chicago Center for Theoretical Chemistry, University of Chicago, Chicago, Illinois 60637, United States;* orcid.org/0000-0001-5227-1396; Email: lgagliardi@uchicago.edu

Omar M. Yaghi − *Department of Chemistry, University of California, Berkeley, California 94720, United States; Kavli Energy Nanoscience Institute and Bakar Institute of Digital Materials for the Planet, Division of Computing, Data Science, and Society, University of California, Berkeley, California 94720, United States; KACST−UC Berkeley Center of Excellence for Nanomaterials for Clean Energy Applications, King Abdulaziz City for Science and Technology, Riyadh 11442, Saudi Arabia;* orcid.org/0000-0002-5611-3325; Email: yaghi@berkeley.edu

Authors

Ha L. Nguyen − *Department of Chemistry, University of California, Berkeley, California 94720, United States; Kavli Energy Nanoscience Institute and Bakar Institute of Digital Materials for the Planet, Division of Computing, Data Science, and Society, University of California, Berkeley, California 94720, United States;* orcid.org/0000-0002-4977-925X

Andrea Darù − *Department of Chemistry, Pritzker School of Molecular Engineering, and Chicago Center for Theoretical Chemistry, University of Chicago, Chicago, Illinois 60637, United States;* orcid.org/0000-0002-0825-2101

Saumil Chheda − *Department of Chemistry, University of California, Berkeley, California 94720, United States; Kavli Energy Nanoscience Institute and Bakar Institute of Digital Materials for the Planet, Division of Computing, Data Science, and Society, University of California, Berkeley, California 94720, United States;* orcid.org/0000-0002-0989-5707

Ali H. Alawadhi − *Department of Chemistry, University of California, Berkeley, California 94720, United States; Kavli Energy Nanoscience Institute and Bakar Institute of Digital Materials for the Planet, Division of Computing, Data Science, and Society, University of California, Berkeley, California 94720, United States;* orcid.org/0000-0003-2680-5221

S. Ephraim Neumann − *Department of Chemistry, University of California, Berkeley, California 94720, United States; Kavli Energy Nanoscience Institute and Bakar Institute of Digital Materials for the Planet, Division of Computing, Data Science, and Society, University of California, Berkeley, California 94720, United States;* orcid.org/0000-0002-8515-9621

Lifen Wang − *Beijing National Laboratory for Condensed Matter Physics, Institute of Physics, Chinese Academy of Sciences, Beijing 100190, China; Songshan Lake Materials Laboratory, Dongguan 530808, China; School of Physical Sciences, University of Chinese Academy of Sciences, Chinese Academy of Sciences, Beijing 101408, China;* orcid.org/0000-0002-8468-5048

Xuedong Bai − *Beijing National Laboratory for Condensed Matter Physics, Institute of Physics, Chinese Academy of Sciences, Beijing 100190, China; Songshan Lake Materials Laboratory, Dongguan 530808, China; School of Physical Sciences, University of Chinese Academy of Sciences, Chinese Academy of Sciences, Beijing 101408, China;* orcid.org/0000-0002-1403-491X

Majed O. Alawad − *KACST−UC Berkeley Center of Excellence for Nanomaterials for Clean Energy Applications, King Abdulaziz City for Science and Technology, Riyadh 11442, Saudi Arabia*

Christian Borgs − *Bakar Institute of Digital Materials for the Planet, Division of Computing, Data Science, and Society and Department of Electrical Engineering and Computer Sciences, University of California, Berkeley, California 94720, United States*

Jennifer T. Chayes − *Bakar Institute of Digital Materials for the Planet, Division of Computing, Data Science, and Society,*

https://doi.org/10.1021/acscentsci.4c01878
ACS Cent. Sci. XXXX, XXX, XXX−XXX

Department of Electrical Engineering and Computer Sciences, Department of Mathematics, Department of Statistics, and School of Information, University of California, Berkeley, California 94720, United States

Complete contact information is available at: https://pubs.acs.org/10.1021/acscentsci.4c01878

Author Contributions

H.L.N. conceived the idea. H.L.N. synthesized and characterized the materials. A.D. performed structure and water sorption simulations. H.L.N., S.C., and A.H.A. analyzed the correlation between water sorption isotherms and COF/MOF structural properties. H.L.N. and A.H.A. collected and interpreted data on water vapor sorption. S.E.N. collected ^{13}C CP-MAS NMR spectra and SEM. L.W. and X.B. collected TEM images. M.O.A., C.B., and J.T.C. discussed the correlation between water sorption isotherms and COF/MOF structural properties. J.S. and L.G. directed the theoretical simulations. O.M.Y. directed and supervised the project. The manuscript was written through contributions of all authors.

Funding

National Science Foundation (NSF), Division of Chemistry, Chemical Structure, Dynamics, and Mechanisms A (CSDM−A) supporting the computational resources, award number: CHE-2223442; Deutsche Forschungsgemeinschaft (DFG, German Research Foundation) − 509313931; NIH S10OD024998; the University of Chicago's Research Computing Center.

Notes

The authors declare the following competing financial interest(s): Omar M. Yaghi is founder of Atoco Inc., aiming at commercializing related technologies. One patent application based on the findings reported in this work has been filed.

■ ACKNOWLEDGMENTS

We acknowledge the National Science Foundation (NSF), Division of Chemistry, Chemical Structure, Dynamics, and Mechanisms A (CSDM−A) supporting the computational resources, award number: CHE-2223442. We thank the Deutsche Forschungsgemeinschaft (DFG, German Research Foundation) − 509313931 for the financial support. We thank the College of Chemistry Nuclear Magnetic Resonance Facility for resources and staff assistance, where instruments are partially supported by NIH S10OD024998. We are also grateful to Dr. Kevin Hunter Stone (the Stanford Linear Accelerator Center, Stanford University, beamline 2-1) for efforts to measure PXRD of COF-309. We acknowledge the University of Chicago's Research Computing Center for providing the resources to carry out this work.

■ ABBREVIATIONS

COFs, covalent organic frameworks; EA, elemental analysis; FT-IR, Fourier-transform infrared spectroscopy; NMR, nuclear magnetic resonance spectroscopy; PXRD, powder X-ray diffraction; TGA, thermogravimetric analysis; SEM, scanning electron microscopy; PXRD, powder X-ray diffraction; TEM, transmission electron microscopy; DFT, density functional theory

■ REFERENCES

(1) Furukawa, H.; Gándara, F.; Zhang, Y.-B.; Jiang, J.; Queen, W. L.; Hudson, M. R.; Yaghi, O. M. Water Adsorption in Porous Metal-Organic Frameworks and Related Materials. *J. Am. Chem. Soc.* **2014**, *136*, 4369−4381.

(2) Canivet, J.; Fateeva, A.; Guo, Y.; Coasne, B.; Farrusseng, D. Water Adsorption in MOFs: Fundamentals and Applications. *Chem. Soc. Rev.* **2014**, *43*, 5594−5617.

(3) Rieth, A. J.; Yang, S.; Wang, E. N.; Dincă, M. Record Atmospheric Fresh Water Capture and Heat Transfer with a Material Operating at the Water Uptake Reversibility Limit. *ACS Cent. Sci.* **2017**, *3*, 668−672.

(4) Nguyen, H. L.; Hanikel, N.; Lyle, S. J.; Zhu, C.; Proserpio, D. M.; Yaghi, O. M. A Porous Covalent Organic Framework with Voided Square Grid Topology for Atmospheric Water Harvesting. *J. Am. Chem. Soc.* **2020**, *142*, 2218−2221.

(5) Tan, K. T.; Tao, S.; Huang, N.; Jiang, D. Water Cluster in Hydrophobic Crystalline Porous Covalent Organic Frameworks. *Nat. Commun.* **2021**, *12*, 6747.

(6) Stegbauer, L.; Hahn, M. W.; Jentys, A.; Savasci, G.; Ochsenfeld, C.; Lercher, J. A.; Lotsch, B. V. Tunable Water and CO_2 Sorption Properties in Isostructural Azine-Based Covalent Organic Frameworks through Polarity Engineering. *Chem. Mater.* **2015**, *27*, 7874−7881.

(7) Nguyen, H. L.; Gropp, C.; Hanikel, N.; Möckel, A.; Lund, A.; Yaghi, O. M. Hydrazine-Hydrazide-Linked Covalent Organic Frameworks for Water Harvesting. *ACS Cent. Sci.* **2022**, *8*, 926−932.

(8) Biswal, B. P.; Kandambeth, S.; Chandra, S.; Shinde, D. B.; Bera, S.; Karak, S.; Garai, B.; Kharul, U. K.; Banerjee, R. Pore Surface Engineering in Porous, Chemically Stable Covalent Organic Frameworks for Water Adsorption. *J. Mater. Chem. A* **2015**, *3*, 23664−23669.

(9) Karak, S.; Kandambeth, S.; Biswal, B. P.; Sasmal, H. S.; Kumar, S.; Pachfule, P.; Banerjee, R. Constructing Ultraporous Covalent Organic Frameworks in Seconds via an Organic Terracotta Process. *J. Am. Chem. Soc.* **2017**, *139*, 1856−1862.

(10) Chen, L.; Han, W.; Yan, X.; Zhang, J.; Jiang, Y.; Gu, Z. A Highly Stable Ortho -Ketoenamine Covalent Organic Framework with Balanced Hydrophilic and Hydrophobic Sites for Atmospheric Water Harvesting. *ChemSusChem* **2022**, *15*, No. e202201824.

(11) Sun, C.; Zhu, Y.; Shao, P.; Chen, L.; Huang, X.; Zhao, S.; Ma, D.; Jing, X.; Wang, B.; Feng, X. 2D Covalent Organic Framework for Water Harvesting with Fast Kinetics and Low Regeneration Temperature. *Angew. Chem., Int. Ed.* **2023**, *62*, No. e202217103.

(12) Nguyen, H. L. Covalent Organic Frameworks for Atmospheric Water Harvesting. *Adv. Mater.* **2023**, *35*, 2300018.

(13) Grunenberg, L.; Savasci, G.; Emmerling, S. T.; Heck, F.; Bette, S.; Cima Bergesch, A.; Ochsenfeld, C.; Lotsch, B. V. Postsynthetic Transformation of Imine- into Nitrone-Linked Covalent Organic Frameworks for Atmospheric Water Harvesting at Decreased Humidity. *J. Am. Chem. Soc.* **2023**, *145*, 13241−13248.

(14) Hanikel, N.; Pei, X.; Chheda, S.; Lyu, H.; Jeong, W.; Sauer, J.; Gagliardi, L.; Yaghi, O. M. Evolution of Water Structures in Metal-Organic Frameworks for Improved Atmospheric Water Harvesting. *Science* **2021**, *374*, 454−459.

(15) Hanikel, N.; Prévot, M. S.; Yaghi, O. M. MOF Water Harvesters. *Nat. Nanotechnol.* **2020**, *15*, 348−355.

(16) Maia, R. A.; Oliveira, F. L.; Nazarkovsky, M.; Esteves, P. M. Crystal Engineering of Covalent Organic Frameworks Based on Hydrazine and Hydroxy-1,3,5-Triformylbenzenes. *Cryst. Growth Des.* **2018**, *18*, 5682−5689.

(17) Geng, K.; He, T.; Liu, R.; Tan, K. T.; Li, Z.; Tao, S.; Gong, Y.; Jiang, Q.; Jiang, D.; Dalapati, S.; Tan, K. T.; Li, Z.; Tao, S.; Gong, Y.; Jiang, Q.; Jiang, D. Covalent Organic Frameworks: Design, Synthesis, and Functions. *Chem. Rev.* **2020**, *120*, 8814−8933.

(18) Hu, J.; Huang, Z.; Liu, Y. Beyond Solvothermal: Alternative Synthetic Methods for Covalent Organic Frameworks. *Angew. Chem., Int. Ed.* **2023**, *62*, No. e202306999.

(19) Fröhlich, D.; Pantatosaki, E.; Kolokathis, P. D.; Markey, K.; Reinsch, H.; Baumgartner, M.; van der Veen, M. A.; De Vos, D. E.;

Stock, N.; Papadopoulos, G. K.; Henninger, S. K.; Janiak, C. Water Adsorption Behaviour of CAU-10-H: A Thorough Investigation of Its Structure-Property Relationships. *J. Mater. Chem. A* **2016**, *4*, 11859−11869.
(20) Cadiau, A.; Lee, J. S.; Damasceno Borges, D.; Fabry, P.; Devic, T.; Wharmby, M. T.; Martineau, C.; Foucher, D.; Taulelle, F.; Jun, C.-H.; Hwang, Y. K.; Stock, N.; De Lange, M. F.; Kapteijn, F.; Gascon, J.; Maurin, G.; Chang, J.-S.; Serre, C. Design of Hydrophilic Metal Organic Framework Water Adsorbents for Heat Reallocation. *Adv. Mater.* **2015**, *27*, 4775−4780.
(21) Jeremias, F.; Fröhlich, D.; Janiak, C.; Henninger, S. K. Advancement of Sorption-Based Heat Transformation by a Metal Coating of Highly-Stable, Hydrophilic Aluminium Fumarate MOF. *RSC Adv.* **2014**, *4*, 24073−24082.
(22) Fathieh, F.; Kalmutzki, M. J.; Kapustin, E. A.; Waller, P. J.; Yang, J.; Yaghi, O. M. Practical Water Production from Desert Air. *Sci. Adv.* **2018**, *4*, No. eaat3198.
(23) Alawadhi, A. H.; Chheda, S.; Stroscio, G. D.; Rong, Z.; Kurandina, D.; Nguyen, H. L.; Rampal, N.; Zheng, Z.; Gagliardi, L.; Yaghi, O. M. Harvesting Water from Air with High-Capacity, Stable Furan-Based Metal-Organic Frameworks. *J. Am. Chem. Soc.* **2024**, *146*, 2160−2166.
(24) Hanikel, N.; Kurandina, D.; Chheda, S.; Zheng, Z.; Rong, Z.; Neumann, S. E.; Sauer, J.; Siepmann, J. I.; Gagliardi, L.; Yaghi, O. M. MOF Linker Extension Strategy for Enhanced Atmospheric Water Harvesting. *ACS Cent. Sci.* **2023**, *9*, 551−557.
(25) Wang, H.; Qian, C.; Liu, J.; Zeng, Y.; Wang, D.; Zhou, W.; Gu, L.; Wu, H.; Liu, G.; Zhao, Y. Integrating Suitable Linkage of Covalent Organic Frameworks into Covalently Bridged Inorganic/Organic Hybrids toward Efficient Photocatalysis. *J. Am. Chem. Soc.* **2020**, *142*, 4862−4871.
(26) Lenzen, D.; Zhao, J.; Ernst, S.-J.; Wahiduzzaman, M.; Ken Inge, A.; Fröhlich, D.; Xu, H.; Bart, H.-J.; Janiak, C.; Henninger, S.; Maurin, G.; Zou, X.; Stock, N. A Metal-Organic Framework for Efficient Water-Based Ultra-Low-Temperature-Driven Cooling. *Nat. Commun.* **2019**, *10*, 3025.
(27) Zheng, Z.; Alawadhi, A. H.; Chheda, S.; Neumann, S. E.; Rampal, N.; Liu, S.; Nguyen, H. L.; Lin, Y.; Rong, Z.; Siepmann, J. I.; Gagliardi, L.; Anandkumar, A.; Borgs, C.; Chayes, J. T.; Yaghi, O. M. Shaping the Water-Harvesting Behavior of Metal-Organic Frameworks Aided by Fine-Tuned GPT Models. *J. Am. Chem. Soc.* **2023**, *145*, 28284−28295.
(28) Oppenheim, J. J.; Dincă, M. Isoreticular Curves: A Theory of Capillary Condensation To Model Water Sorption within Microporous Sorbents. *J. Am. Chem. Soc.* **2024**, *146*, 20615−20626.
(29) Zaragoza, A.; Factorovich, M. H.; Molinero, V. Multistage Condensation Pathway Minimizes Hysteresis in Water Harvesting with Large-Pore Metal-Organic Frameworks. *Chem. Mater.* **2024**, *36*, 708−719.

https://doi.org/10.1021/acscentsci.4c01878
ACS Cent. Sci. XXXX, XXX, XXX−XXX